Available online at www.sciencedirect.com
ScienceDirect
Journal of Catalysis 248 (2007) 60–67
JOURNAL OF CATALYSIS
www.elsevier.com/locate/jcat

TAP study on carbon monoxide oxidation over supported gold catalysts $Au/Ti(OH)_4^*$ and $Au/Fe(OH)_3^*$: Moisture effect

Maria Olea *, Mizuki Tada, Yasuhiro Iwasawa

Department of Chemistry, Graduate School of Science, The University of Tokyo, Hongo, Bunkyo-ku, Tokyo 113-0033, Japan

Received 27 December 2006; revised 6 March 2007; accepted 6 March 2007

Abstract

The effect of moisture on the behavior of the active supported gold catalysts developed by us, $Au/Ti(OH)_4^*$ (I) and $Au/Fe(OH)_3^*$ (II), during CO activation and CO oxidation in the temperature range 298–473 K was investigated by the temporal analysis of products (TAP) technique. The oxidation reaction over the $Au/Ti(OH)_4^*$ catalyst was totally suppressed by the presence of water, independent of the water content of 200 and 1000 ppm, the carbon monoxide-to-oxygen ratio, and the temperature. In contrast, the presence of water vapors showed no effect on CO oxidation over the $Au/Fe(OH)_3^*$ catalyst. For both catalysts, the carbon monoxide adsorption feature was unalterable by the presence of water, namely CO molecules reversibly adsorbed on the catalyst surface, but the amount of CO adsorbed decreased by increasing water content. When a reaction mixture at a 1:1 ratio of CO to O_2 was pulsed on the catalyst in the absence of water, the CO response curve showed two peaks, whereas in the presence of water, the TAP response curve showed only one peak. At a 1:3 CO-to-O_2 ratio, the CO response curve showed only one peak, which shifted to a shorter time and narrowed in the absence of water. The shift was more pronounced on catalyst (II). The TAP experiments provided indirect evidence that CO and water adsorbed together (CO weakly and water strongly) and water blocked [irreversibly for $Au/Ti(OH)_4^*$ and reversibly for $Au/Fe(OH)_3^*$], the adsorption sites for oxygen.

Keywords: Supported gold catalyst; Carbon monoxide oxidation; Reaction mechanism; Moisture effect; TAP study

1. Introduction

Supported gold nanoparticle catalysts have received intense and broad interests since the report of Harada et al. [1] of their high catalytic activity for low-temperature CO oxidation. Increasing efforts in both catalytic and industrial chemistry [2–12] and cluster and theoretical science [13–15] have been devoted to clarifying the origins of the unique catalytic properties. These properties have been related to changes in the electronic properties, the presence of defect sites, and the existence of strain for metallic gold nanoparticles [16–20]. Unique catalytic properties also have been related to the presence of sites associated with the catalyst support, such as cationic gold species, and sites at gold–support interfaces [21,22]. The size of Au particles [2,3], the nature of the support [23,24], the methods of preparation and pretreatment [25], and the operating environment have been proposed to be critical to the high activity. Despite previous efforts, however, there are still some uncertainty and debate concerning the precise mechanism of the CO oxidation over these catalysts and the effect of moisture on the catalytic performance of gold.

To date, there have been several reports, sometimes contradictory, about the effect of moisture on supported gold catalysts. Daté and Haruta [26] reported that moisture enhanced the reaction by more than 10 times up to 200 ppm H_2O, and further increases in moisture content suppressed the reaction over an Au/TiO_2 catalyst obtained by deposition–precipitation. At low moisture content, the positive effect was attributed to a change in the amount of water-derived species, which may activate O_2 molecules or modify the electronic state of gold atoms exposed at the surface. At high moisture content, the suppression of catalytic activity was purportedly due to the adsorption of water

* Corresponding author. Present address: Laboratorium voor Petrochemische Techniek, Ghent University, Krijgslaan 281 S5, 9000 Ghent, Belgium. Fax: +32 9 264 4999.
E-mail address: maria.olea@ugent.be (M. Olea).

0021-9517/$ – see front matter
doi:10.1016/j.jcat.2007.03.004

on oxygen vacancies, which were then blocked for further adsorption of O_2.

Augmentation of the oxidation activity in the presence of water was reported for Au/Fe_2O_3 [27,28], Au/Al_2O_3 [28,29], and $Au/Mg(OH)_2$ [30] catalysts obtained by a deposition–precipitation method. Bond et al. [31] proposed a possible reaction mechanism for CO oxidation that involves hydroxyl species. On the other hand, enhancement of activity by the adsorbed water species was explained by the prevention of the reduction of cationic gold species for those catalysts with active sites consisting of cationic Au^+ with a hydroxyl ligand and neighboring metallic Au atoms [29,32].

For an impregnated Au/TiO_2 catalyst, the presence of water was found to suppress the catalytic activity [33]. The deactivation of the impregnated Au/TiO_2 catalyst by water vapor may be due to H_2O adsorption on TiO_2, because water is known to adsorb both associatively and dissociatively (as OH^-) on reduced Ti cations and to oxidize the surface [34], thus blocking the coordinatively unsaturated sites at the TiO_2 surface.

Iwasawa and coworkers developed iron and titanium oxide-supported gold catalysts, $Au/Fe(OH)_3^*$ [35,36] and $Au/Ti(OH)_4^*$ [37], derived from Au–phosphine complex precursor for Au particles and as-precipitated $M(OH)_x^*$ precursors for metal oxide supports, that were very active for CO oxidation, and reported that coexisting water vapor showed no effect and a negative effect, respectively. Based on FT-IR spectra of CO adsorbed on $Au/Fe(OH)_3^*$ in the presence of various H_2O pressures [35], the insensitivity of this catalyst to water vapor was linked to the presence of water, which greatly inhibited CO adsorption on Fe^{3+} and dissociatively adsorbed on oxygen vacancies of the Fe-oxide surface and reacted with CO to form CO_2 by the water-gas shift reaction. Thus, the oxygen vacancies were recovered to be available for O_2 adsorption. To explain the different behavior of the $Au/Ti(OH)_4^*$ catalyst, additional experiments were envisaged [35]. The key step seems to be CO adsorption.

A careful analysis of literature data leads to the conclusion that the effect of water on the activity of supported gold catalysts depends on the method of preparation, the nature of the support, and the Au particle size, dispersion, and oxidation state.

In the present study, the TAP technique was used to further investigate the different effect of water on the CO oxidation over the two catalysts, $Au/Ti(OH)_4^*$ (I) and $Au/Fe(OH)_3^*$ (II). TAP is a technique sensitive to each step in a heterogeneous catalytic process. We previously reported TAP studies [38,39] on the diffusion and adsorption of carbon monoxide, oxygen, and carbon dioxide adsorption/desorption, as well as catalytic carbon monoxide oxidation over the titania-supported gold catalyst (I), with all studies performed in the absence of moisture. We found that carbon monoxide molecules reversibly and weakly adsorbed on the catalyst surface; oxygen adsorbed molecularly and strongly for high pulse intensities, with lifetimes of 4500–6900 ms at 373–423 K; reaction occurred between adsorbed carbon monoxide and adsorbed molecular oxygen; and lattice oxygen atoms were active in oxygen exchange only with carbon dioxide. TAP results confirmed the carbon monoxide oxidation mechanism on the catalysts previously reported by Iwasawa's group [35,37].

The main goal of the present paper is to reveal those details of the CO adsorption mechanism and features that provide insight into the influence of water on CO oxidation activity over $Au/Ti(OH)_4^*$ (I) and $Au/Fe(OH)_3^*$ (II) catalysts. For this purpose, single-pulse TAP experiments were performed to investigate the diffusion of Ar and He and the adsorption of CO (dry and moisturized) and O_2. Pump-probe (or alternating) TAP experiments were conducted to explore the behavior of the fresh or oxygen precovered catalysts. The O_2 pump molecule was probed with both dry and moisturized CO at different time intervals to provide information about the reactive surface species and individual reaction steps. All TAP experiments in the presence of water were performed at the same temperatures as previously done in the absence of water: 298, 373, and 473 K. This allowed a direct comparison of the data and a clear assessment of the effect of water.

2. Experimental

All experiments were conducted using a TAP reactor system as described in detail elsewhere [38,39]. Briefly, the setup consisted of a catalytic microreactor, a gas delivery system for introduction of either high-speed gas pulses or a continuous flow of gas, a high throughput, a high-vacuum system, and a computer-controlled quadrupole mass spectrometer. The microreactor was a stainless steel tube 2 mm in diameter and 25 mm long. Catalyst samples of 0.024 g were used in these experiments, resulting in catalyst bed length of 10 mm. Throughout the study, the 250–425 μm fraction was loaded and fixed in the reactor by stainless steel mesh. The reactor could be heated up to 773 K by cartilage heaters. The two high-speed pulse valves could be operated at intervals of up to 50 pulses s^{-1}. The minimum pulse width was 200 μs. The pulse intensities were varied between 10^{13} and 10^{18} molecules per pulse, allowing the transport in the reactor to occur through Knudsen diffusion. Before each experiment, the catalyst was heated up to 473 K for 30 min in vacuum to desorb preadsorbed species. To increase the signal-to-noise ratio in the response, 25 pulses per atomic mass unit (AMU) value were monitored and averaged. Alternating and simultaneous pulsing experiments were carried out using 1:1 He/CO (dry or moisturized) mixture in one valve and 1:1 He/O_2 mixture in the second valve. For dry experiments, the two feeding mixtures were purified by being passed through a silica trap at a dry ice-acetone temperature. The concentrations of moisture in CO gas phase were 200 and 1000 ppm, and the resulting mixtures were designated CO_{m2} and CO_{m10} to differentiate them from the dry CO. These two particular moisture values were chosen because they were found to be threshold amounts for the enhancement and suppression, respectively, of catalytic activity over an Au/TiO_2 catalyst obtained by a deposition–precipitation method [26].

For each experiment, the conversion was calculated according to the following equation:

$$X_i = \frac{n_{\mathrm{in},i} - n_{\mathrm{out},i}}{n_{\mathrm{in},i}}, \tag{1}$$

where n is the total number of mol and X is the conversion for component i, CO or O_2 (mol mol^{-1}). The subscript "in" means introduced into the reactor, and the subscript "out" means detected at the reactor outlet. Using He as an internal standard allows a precise determination of the number of molecules at the reactor outlet. No influence on catalytic activity was found when the catalysts were kept for one night under vacuum at the highest temperature used during experiments. Because the water–gas shift reaction could occur on these catalysts, hydrogen production was assessed by monitoring the changes in the background spectra at AMU of 2 before and after the CO oxidation reaction. Virtually no differences at AMU of 2 were found before and after the oxidation reaction.

The catalysts were prepared as described in detail elsewhere [35–37,40]. As-precipitated wet metal hydroxides, $M(OH)_x^*$, were obtained by hydrolysis of $M(O^iC_3H_7)_x$ (99.999% purity) with an aqueous solution containing 5% of Na_2CO_3 (99.9% purity). The precipitates were then filtrated and washed with deionized water to pH 7.0. The as-precipitated wet $M(OH)_x^*$ was impregnated with an acetone solution of $Au(PPh_3)(NO_3)$ under vigorous stirring, followed by vacuum drying to remove the solvent at room temperature. The sample thus obtained was heated to 673 K at a ramp rate of 4 K min^{-1} and kept at this temperature for 4 h in a flow of air (30 ml min^{-1}). Calcination of the samples led to decomposition of both precursors, $Au(PPh_3)(NO_3)$ and $M(OH)_x^*$, to metallic Au particles and TiO_2 and Fe_2O_3, respectively. EXAFS measurements in a transmission mode carried out at Au L_3-edge before and after calcination indicated the formation of Au particles. The average Au particle size estimated by transmission electron microscopy was 2.9 nm for $Au/Fe(OH)_3^*$ and 6.6 nm for $Au/Ti(OH)_4^*$. The change in the Au species from the phosphine complex to metallic particles was accompanied by the development of the XRD peaks for crystalline TiO_2 and Fe_2O_3 [40–42]. The catalysts thus obtained are denoted as $Au/M(OH)_x^*$ where the term $M(OH)_x^*$ is used only to clarify the origin of metal oxide, discriminating the preparation of the hydroxide-based gold catalysts from that of conventional Au/TiO_2 and Au/Fe_2O_3 catalysts obtained by an incipient wetness impregnation method. The Au loading on both supports was controlled at 3.0 wt% [41]. The use of as-precipitated wet $M(OH)_x^*$ as precursors was decisive in obtaining the highly active catalyst [35–37,40–42].

3. Results and discussion

The catalysts used in this study were very active for CO oxidation in the absence of moisture. In contrast, in the presence of moisture, the catalytic activity was totally suppressed for catalyst (I) and remained unchanged for catalyst (II). To understand the different behavior of the two catalysts in the presence of water, single-pulse and alternating-pulse TAP experiments were performed, and the TAP response curves were analyzed.

3.1. Gas transport

Four single-pulse experiments with inert gases He and Ar were performed at 298, 373, and 473 K to determine the pulse intensity window for Knudsen diffusion only. Following the procedure described previously [38], it was found that for pulse intensities below 1×10^{18} molecules/pulse, the gas transport through the catalyst bed fitted perfectly the Knudsen diffusion flow for nonporous catalysts. The average values for He and Ar effective Knudsen diffusivities were 0.443 and 0.140 cm^2 s^{-1}, respectively, considering an average porosity of bed of 0.23. The effective Knudsen diffusivities for CO and O_2 reactant gases against He were 0.167 and 0.156 cm^2 s^{-1}, respectively. The low content of moisture in the CO gas phase induced no significant difference in the effective diffusivity of CO.

We performed experiments with the two inert gases, which had significantly different molecular masses, to assess the intraparticle Knudsen diffusion as if it would have been the case. But this in fact was not the case, and, because our catalyst behaves like a nonporous catalyst, we chose to report results relative to He only.

3.2. CO and O_2 adsorption

The interaction of CO and O_2 with the $Au/M(OH)_x^*$ catalysts was investigated through CO and O_2 TAP single-pulse experiments. Fig. 1 shows the CO, CO_{m10}, CO_{m2}, O_2, and He area normalized responses obtained when 25 pulses of CO, CO, CO_{m10}, CO_{m2}, and O_2 in He were passed on catalyst (I) at 298 K. The normalized responses at 373 and 473 K have similar shapes, with the only difference in the position of the cross point, as explained below. Comparing the shape of the responses for the reactant gases with that for He, we concluded that irrespective of the concentration of moisture and temperature, CO reversibly adsorbed on the surface, because the CO response curves crossed the He curve. On the other hand, O_2 showed an irreversible adsorption at all temperatures, with the O_2 response curves under the He response curve [43]. The CO intersection point shifted to a shorter time with increased moisture content in CO at 298 K. The difference grew smaller with increasing temperature, and there was almost no difference at

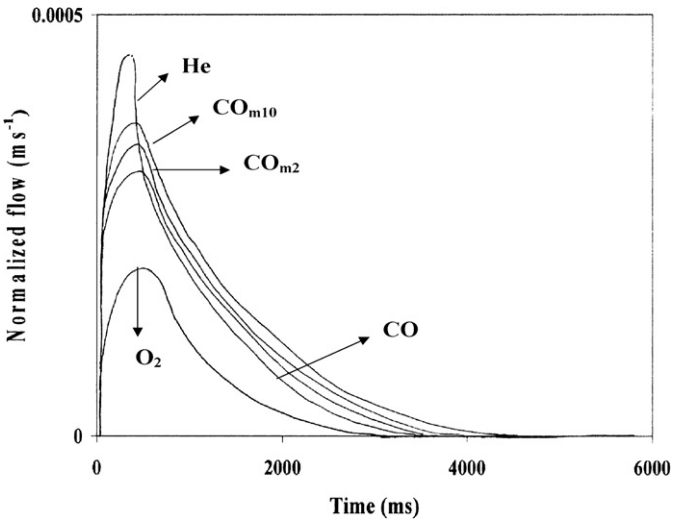

Fig. 1. Area normalized responses at 298 K on 0.024 g $Au/Ti(OH)_3^*$ catalyst for He, CO, CO_{m10}, CO_{m2}, and O_2.

Table 1
Mean apparent adsorption rate constants for CO, CO_{m2}, and CO_{m10}, at 298, 373, and 473 K, respectively, and standard deviations

Adsorption rate constant (s^{-1}) and (σ)/species	Temperature (K)		
	298	373	473
CO	0.014 (0.0003)	0.021 (0.0004)	0.026 (0.0006)
CO_{m2}	0.010 (0.0005)	0.018 (0.00055)	0.025 (0.0008)
CO_{m10}	0.007 (0.0006)	0.013 (0.0007)	0.024 (0.0009)

473 K. The shift of the intersection point to shorter times can be explained as follows. For a reversible adsorption, the time position at which the reversible adsorption and inert gas response curves intersect depends on the adsorption and desorption rate constants. The adsorption rate depends partly on the concentration of adsorption sites at the surface. If some of the active sites are occupied with water, then the concentration of active sites available for CO adsorption decrease and thus the apparent adsorption rate constant decreases, and in this case the influence of desorption on the intersection point becomes less significant, leading to a shorter time of the intersection point.

Analysis of the zeroth, first, and second moments of the CO TAP curves led to simple relations who were used to calculate adsorption and desorption rate constants [38]. Table 1 presents the apparent adsorption rate constants for the adsorption of CO, CO_{m2}, and CO_{m10}, at 298, 373, and 473 K, respectively. The apparent rate constants increase with temperature for all three species considered, and at a constant temperature they decrease slightly with increasing water content in the moisture. At 473 K, only slight differences in the CO apparent adsorption rate constants are seen for dry CO and the two moistures.

But are these small differences between values of apparent adsorption rate constants really significant, or are they due to experimental uncertainties? To explore this question, the experiments were repeated three times for each temperature and CO mixture. In all cases, the standard deviation was less than the difference between the values of apparent adsorption rate constants. As a general tendency, the standard deviation of all samples in a pulse response was lower at lower temperature. The level of noise was higher with higher amounts of water in the CO mixture.

For the catalyst (II), the adsorption of CO in the absence and presence of water and O_2 adsorption show the same features as for the catalyst (I). The only difference was in the time position at which the CO curve intersects the He curve, which was shifted to longer time. At 298 K, the time position of the intersection of the two curves was shifted 300 ms; in this case, the apparent adsorption rate constant was 1.5 times higher than on catalyst (I). Similarly, we can conclude that the shift of the intersection point to longer time is due to the existence of a higher concentration of active sites for CO adsorption on catalyst (II). The apparent adsorption rate constant, k'_a, is defined by:

$$k'_a = \frac{a_s S_V (1-\varepsilon_b) k_a}{\varepsilon_b}, \tag{2}$$

where a_s is surface concentration of active sites (mol cm^{-2} of catalyst), S_V is surface area of catalyst per volume of catalyst (cm^{-1}), ε_b is porosity of the bed, and k_a is adsorption rate constant (cm^3 of gas mol^{-1} s^{-1}). The parameter a_s can be extracted from the value of k'_a at given values of k_a and S_V. Therefore, TAP single-pulse experiments evidenced the fact that the concentration of active sites available for CO adsorption is lower on catalyst (I) than on catalyst (II) and also show that water and part of CO should adsorb on the same type of adsorption sites as the concentration of active sites available for CO adsorption decreases by increasing the water content. Thus, competitive adsorption of H_2O and CO may occur on both catalysts.

To determine how strongly the water was adsorbed on the two catalysts, the TAP single-pulse experiments on CO adsorption in the absence of water were repeated after pulsing He over the catalysts for 30 min. Whereas for catalyst (II), the former position of CO intersection time with He curve was recovered, for catalyst (I), the new intersection time of dry CO with the He curve was shifted to shorter times (about 50 ms at 298 K, 35 ms at 373 K, and about 20 ms at 473 K). On other words, on catalyst (II), the adsorption of water seems to be weak and reversible, whereas for catalyst (I), stronger and irreversible adsorption of water seems to occur.

Concerning the oxygen responses at a pulse intensity of about 1×10^{16} molecules/pulse, an irreversible adsorption occurs on both catalysts. Fig. 1 shows the O_2 adsorption features for catalyst (I) at 298 K. The normalized responses at 373 and 473 K follow the same trend as that at 298 K. The amount of adsorbed oxygen increases with increasing temperature up to 373 K. Following the procedure described in [38], the oxygen was found to adsorb molecularly, and the conversion was estimated to be 13% at 298 K and 26% at 373 K, whereas at 473 K, the oxygen conversion decreased at 11%. We roughly calculate apparent activation energy to be 11 kJ mol^{-1} from room temperature to 373 K. For catalyst (II), more oxygen was adsorbed: 14.5% at 298 K, 29% at 373 K, and about 12.5% at 473 K, and the apparent activation energy was around 7.5 kJ mol^{-1}, which implies a weaker interaction of adsorbed oxygen with Fe^{2+} oxygen vacancy sites. In addition, O_2-TPD experiments suggested that of all the adsorbed oxygen species on catalyst (I) and (II) are active for CO oxidation at room temperature [35].

To explain the maximum conversion at 373 K, the following mechanism of the oxygen adsorption was proposed:

$$O_2 + Y \Leftrightarrow O_2Y \xrightarrow{+e^-} O_2\text{-}Y.$$

At low pulse intensities, only reversible physical adsorption occurs. In this case, the oxygen-adsorbed species could be considered a mobile precursor for the oxygen chemisorption. If a molecule adsorbs in the precursor state, it may (i) become chemisorbed, (ii) be inelastically scattered back into the gas phase, or (iii) hop to a neighboring site, in which case pathways (i) and (ii) are again open. For high pulse intensities, as those used within this study, the oxygen chemisorption becomes competitive with the oxygen desorption. Previous experimental results have indicated that significant changes in the shape of the TAP response curves occur when differences in conversions are at least 9%. Because for both catalysts, the differences in conversion from 298 to 373 K were >9%, we concluded that these

data are significant and thus the activation energies for the two catalysts can be differentiated.

Now the problem is to determine the nature of adsorption sites on which the competitive adsorption of CO and water occurs. On the Au/Ti(OH)$_4^*$ catalyst, three CO adsorption sites were characterized by FT-IR spectra at $\nu_{CO} = 2119$, 2136, and 2188 cm^{-1}. The band at 2188 cm^{-1} was assigned to linear CO on Ti^{4+}, the band at 2119 cm^{-1} was assigned to linear CO on Au metallic particles, and the band at 2136 cm^{-1} was tentatively assigned to CO on Au particles strongly interacting with the support surface. For the Au/Fe(OH)$_3^*$ catalyst, only two bands were observed, at 2170 and 2137 cm^{-1}. The band at 2170 cm^{-1} can be assigned to linear CO on Fe^{3+}, whereas the higher-frequency ν_{CO} peak at 2137 cm^{-1} may be attributed to probably more finely dispersed Au particles compared with Au particles in the Au/Ti(OH)$_4^*$ catalyst [35,37]. The smaller size of Au particles in Au/Fe(OH)$_3^*$ compared with Au/Ti(OH)$_4^*$ was confirmed by the Au coordination number derived from EXAFS analysis (7.4 ± 1 and 9.8 ± 1, respectively) [36,40]. The former studies demonstrated that the CO molecules reversibly adsorbed on Au particles and irreversibly on the metal oxide support surfaces, and that only those adsorbed on Au particles strongly interacting with the support surface contributed to the catalytic CO oxidation [35,37]. Therefore, on both catalysts, a part of CO is expected to adsorb on oxygen vacancies of the support. The finding of a reversible adsorption feature of CO on the TAP experiment most likely indicates that CO adsorbs preferentially on Au nanoparticles, with only a small amount of CO adsorbing on M sites. The more Au nanoparticles on the catalyst surface, the greater the CO adsorption.

Moreover, it is highly likely that at low temperature, the dissociative adsorption of water occurs on coordinatively unsaturated M sites that are available for CO adsorption. Increasing the temperature will likely cause desorption of water from the surface, making the M sites available for CO adsorption once again. At 298 K, the number of CO molecules pulsed over the catalyst in a single-pulse experiment was around 2.5×10^{17}. For the CO_{m10} mixture, the number of water molecules pulsed together with CO was 2.5×10^{14}; for the CO_{m2} mixture, it was 5×10^{13}. Because the catalyst surface has about 10^{20} Ti^{4+} and about the same number of Fe^{3+} sites per gram, the number of M^{x+} sites for a 0.024-g catalyst loading is about 2.4×10^{18}. If all of these sites would have been available for the adsorption of water, then the amount of adsorbed water would have been as little as 0.01% of the exposed M^{x+} ions for the CO_{m10} mixture and 0.002% for the CO_{m2} mixture. These values are too low to explain the difference in CO adsorption as a function of the moisture concentration. More likely, water adsorbs only on coordinatively unsaturated $M^{(x-1)+}$ sites adjacent to oxygen vacancies, which are as little as 1% of the exposed M^{x+} ions.

On the other hand, ESR spectra show that O_2 also adsorbed on those sites to form Ti^{4+}–O_2^- species, which may be located more at the gold interface [37]. The amount of oxygen adsorbed on the catalyst (I) was 3.1 μmol g^{-1} [37], meaning that the number of the Ti^{3+}-oxygen vacancy sites is 1.9×10^{18} sites g^{-1}, or 4.56×10^{16} sites in the TAP reactor. In this case, water can adsorb on 0.5% of the Ti sites at the surface for the CO_{m10} mixture and 0.1% of the Ti sites for the CO_{m2} mixture.

Taking into account all of these findings, we can assume competitive adsorption of a part of CO and water on the Ti^{3+}-oxygen vacancy sites situated at the gold interface, where oxygen has the highest probability to adsorb as well. At low temperature, water, as a polar molecule, has a higher adsorption probability. Thus, these sites will be blocked for CO adsorption, and the total amount of adsorbed CO will decrease with increasing water content.

For catalyst (II), an increased amount of adsorbed oxygen (3.5 μmol g^{-1}) was found [37]. This indicates a slightly increased number of Fe^{2+}oxygen vacancies at the surface than of Ti^{3+} oxygen vacancies, that is, 2.1×10^{18} sites g^{-1}.

3.3. CO–O_2 reaction

A series of experiments for CO–O_2 reactions were performed in which dry and moisturized carbon monoxide and oxygen were pulsed over the Au/Ti(OH)$_4^*$ (I) and Au/Fe(OH)$_3^*$ (II) catalysts, either simultaneously or at various time intervals between the reactant pulses. Fig. 2 shows the normalized response of CO when the two reactants CO and O_2 (at a 1:1 ratio) were pulsed simultaneously at 298 K, along with the He response, over catalyst (II). The normalized response of CO from a CO pulse at 298 K is also shown for comparison, providing a better understanding of the behavior of the catalyst during reaction. Even at this low temperature, the catalysts shows high activity for CO oxidation. The CO conversion was 45% and increased to 52% at 473 K for (I) and was between 50 and 79% for (II). As expected, the TAP conversions are lower than those obtained under steady-state conditions in a fixed-bed flow reactor, in which larger amounts of catalysts were used, that is, 0.200 g instead of 0.024 g.

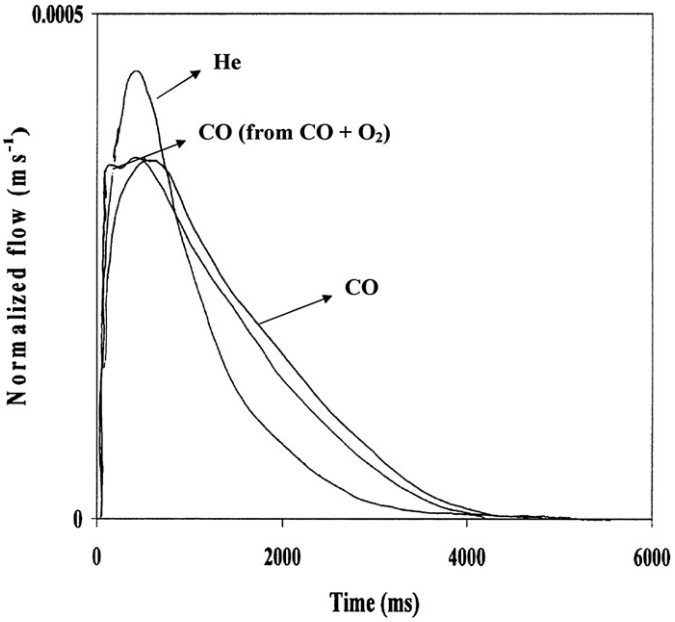

Fig. 2. Area normalized responses at 298 K on 0.024 g Au/Fe(OH)$_3^*$ catalyst for He, CO from CO single-pulses and CO from simultaneous CO + O_2 pulse.

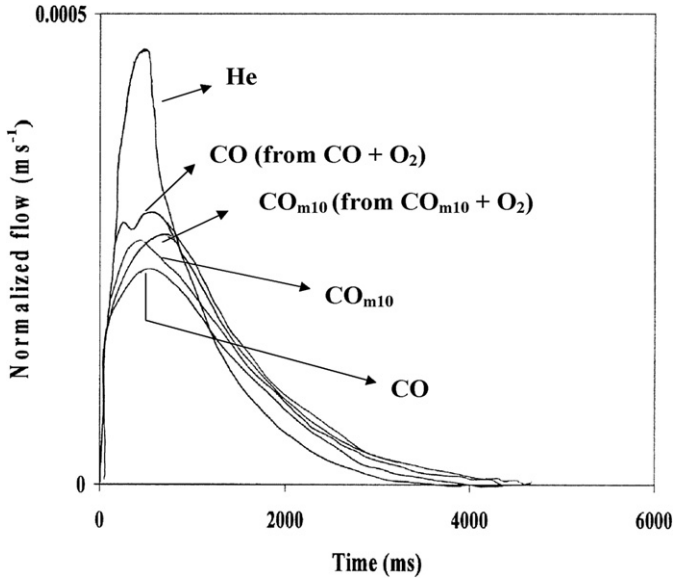

Fig. 3. Area normalized responses at 473 K on 0.024 g Au/Ti(OH)$_4^*$ catalyst for He, CO from CO single-pulses, CO from simultaneous CO + O_2 pulse, CO_{m10} from CO_{m10} single-pulses, and CO_{m10} from simultaneous CO_{m10} + O_2 pulse.

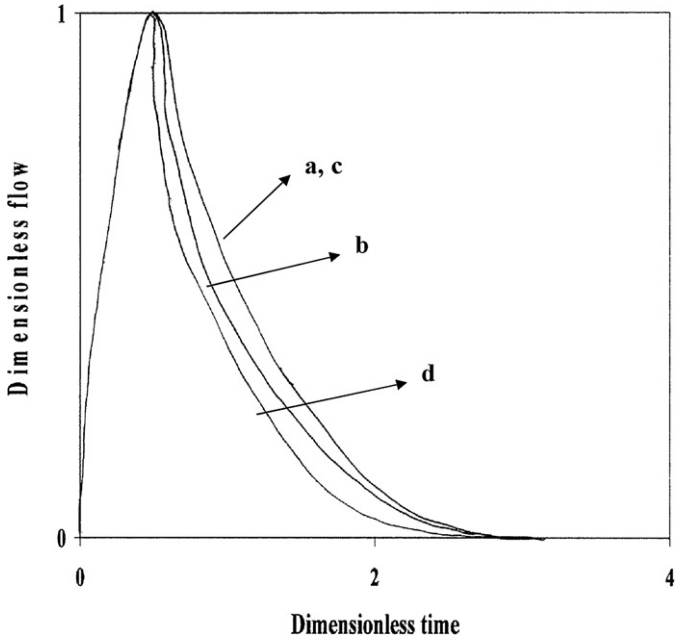

Fig. 4. Dimensionless responses at 373 K on 0.024 g Au/Ti(OH)$_4^*$ catalyst (a and b) and on 0.024 g Au/Fe(OH)$_3^*$ catalyst (c and d) for CO_2: a and c in the CO_2 pulse, b and d in the CO + O_2 pulse.

On both catalysts, the shape of the CO response was different from that obtained when CO alone was pulsed. The reactant curve shifts to shorter time and became slightly narrower. Moreover, after very careful analysis, we concluded that CO as a reactant gives a response curve with two peaks. The two peaks can be hardly distinguished at this temperature, but by increasing the temperature to 473 K, the peaks are more pronounced as shown in Fig. 3. Both peaks show their maxima at shorter times than that of CO alone, which suffers only adsorption on the catalyst surface. Taking into account the findings related to the adsorption of CO, we can assign the first peak from CO response to the CO which attempted to adsorb on the same sites as oxygen and from which it was forced to desorb earlier because O_2 adsorption is stronger than CO adsorption. More CO seems to be adsorbed on other types of adsorption sites, as demonstrated by the presence of the second peak in the CO response.

Fig. 3 also shows the responses of CO_{m10} over catalyst (I) when CO_{m10} was pulsed simultaneously with O_2 at a 1:1 ratio or alone at 473 K. The only difference between the two curves is the shift to shorter times for CO_{m10} pulsed simultaneously. The same behavior was found at the other two temperatures studied, as well for the CO_{m2} mixture. Moreover, no reaction product was detected when water was present in the reactant mixture. The suppression of CO_2 production by water vapor was also observed in the catalytic oxidation in a closed circulating system. Therefore, the shifts in the CO_{m10} and CO_{m2} responses are due only to the forced earlier CO desorption in the presence of O_2.

For catalyst (II), the CO adsorption features when CO dry and O_2 were pulsed simultaneously were similar to those observed over catalyst (I), but the maxima appeared earlier. Another difference in the behavior of catalyst (II) was the finding that the presence of water, irrespective of its content, did not affect catalyst activity. Virtually the same conversion of CO was obtained in the absence and the presence of water.

The CO_2 adsorption/reaction features over the two catalysts were well characterized by comparing the formation of CO_2 from the single-pulse of the 1:1 mixture of CO and O_2 with the TAP response of CO_2 pulse (see Fig. 4). The dimensionless CO_2 response curve for the CO_2 pulse at 373 K was almost similar over the two catalysts. Slightly slower CO_2 desorption can be seen over catalyst (I). In contrast, at the same temperature, the CO_2 response curve for the CO + O_2 pulse over catalyst (II) is sharper than that over catalyst (I). This means that the CO_2 formation rate is higher on the Au/Fe(OH)$_3^*$ catalyst.

Next, alternating pulse experiments were performed at 373 K over catalyst (I). O_2 was pulsed first from the pump valve and then interrogated with the CO pulse from the probe valve at time intervals varying from 50 to 10 000 ms. The reaction product, CO_2, was monitored as a function of the time interval between the two pulses. When dry CO was used as the probe molecule, CO_2 formation increased rapidly with increasing time interval, reaching a maximum at an interval of 1000 ms. CO_2 yield decreased with further increases in the time interval and almost vanished after a 6000-ms interval. These findings demonstrate the participation of the adsorbed oxygen and rule out the possibility that lattice oxygen atoms of the catalyst contribute to the oxidation reaction. When CO_{m10} or CO_{m2} was the probe mixture, no reaction product was observed irrespective of time interval.

The experimental procedure was repeated for a mixture of CO and O_2 at a 1:3 ratio. When CO and O_2 were pulsed simultaneously, the CO response showed only a single peak on both catalysts, which shifted to shorter time and narrowed compared with the CO response for adsorption only. For example, over catalyst (I), the time shift decreased with increasing temperature, from 500 ms at 298 K to 300 ms at 473 K. CO conversion was 50% at 298 K and 56% at 473 K for catalyst (I), with higher

conversions obtained on catalyst (II): 53% at 298 K and 82% at 473 K. This finding was expected. Increasing the amount of oxygen pulsed over the catalyst caused an increase in the number of active M sites occupied with O_2 at the expense of CO. The greater the quantity of oxygen adsorbed on the $M^{(x-1)+}$ oxygen vacancy sites at the support–gold interface, the higher the reaction probability; in other words, the shape of the CO response curve is increasingly determined by the reaction rate.

No reaction product was detected in the presence of moisture, irrespective of water content and temperature over catalyst (I). Comparing CO_{m10} and CO_{m2} responses resulting from the simultaneous pulse with oxygen or from their single pulses over catalyst (I) demonstrated a shift to the shorter time in the presence of oxygen. But the time shift was constant within the temperature range, supporting the assumption that in the presence of oxygen, CO is forced to desorb earlier.

3.4. *Au/Ti(OH)$_4^*$ versus Au/Fe(OH)$_3^*$*

TAP experiments revealed that the CO oxidation reaction on the Au/Ti(OH)$_4^*$ catalyst was totally suppressed by the presence of moisture (200 or 1000 ppm) and that water had no effect on the activity of the Au/Fe(OH)$_3^*$ catalyst. Previous experiments also showed the poisoning effect of water on the catalyst (I) and the insensitivity of catalyst (II) to the presence of moisture [35–37]. TAP also showed that whereas on catalyst (II), the adsorption of water seems to be weak and reversible, on catalyst (I), strong and irreversible adsorption of water seems to occur.

Moreover, in the absence of water, TAP confirmed that the Au/Fe(OH)$_3^*$ catalyst is more active than the Au/Ti(OH)$_4^*$ catalyst. Other studies have shown that the temperature needed to start CO oxidation is 50 K lower for the Au/Fe(OH)$_3^*$ catalyst than for the Au/Ti(OH)$_4^*$ catalyst, whereas the temperatures for 50 and 100% conversions are lower by 100 and 160 K, respectively [40]. The question is why these two catalysts behave differently, given that they were prepared and pretreated in the same way and had the same gold content (3 wt%). Experimental results to date have confirmed the same mechanism for CO oxidation on the two catalysts [35,37]. This mechanism involves reversible CO adsorption on the Au nanoparticle surface; O_2 molecular adsorption, probably as O_2^- bonded to Ti or Fe ions as indicated by ESR [36] on oxygen vacancies on the oxide support near to the Au nanoparticles; and subsequent reaction between the adsorbed CO and O_2^- to form a CO_2 molecule and an active oxygen atom, which rapidly reacts with CO to form another CO_2 [35,37].

The efficiency of supported gold catalysts depends on gold dispersion and the gold–support interaction on one hand, and on the nature, crystalline type, and pore structure of metal oxide supports, on the other hand. The catalytic activity may change by several orders of magnitude due to the effect of the Au–Au coordination number, making this effect dominant and crucial for catalysis by Au [44]. More CO that may adsorb on the Au nanoparticles is seen on the Au/Fe(OH)$_3^*$ catalyst than on the Au/Ti(OH)$_4^*$ catalyst. On the other hand, as the size of the Au nanoparticles decreases, the number of the O_2 adsorption sites at the gold–oxide support interface increases. Oxygen vacancies on TiO_2 and Fe_2O_3 are electrically compensated for by the formation of Ti^{3+} and Fe^{2+}, on which O_2 adsorbs to form Ti^{4+}–O_2^- species and Fe^{3+}–O_2^- species. The former species is more stable than the latter species. Indeed, the temperature peak in TPD of oxygen adsorbed on the Au/Fe(OH)$_3^*$ catalyst, 400 K, was 50 K lower than that for the Au/Ti(OH)$_4^*$ catalyst [35]. The stronger adsorption of O_2 on the Ti(OH)$_4^*$ support may lead to the lower reactivity with CO.

To explain the different behavior of the two catalysts in the absence and presence of water, the support effect also should be considered. In our opinion, the difference in the electronegativity of their cations from the supports is responsible for the stronger dissociative adsorption of water on the Au/Ti(OH)$_4^*$ catalyst, which leads to lower reactivity to adsorbed CO to form CO_2 by the water–gas shift reaction. The water–gas shift reaction is more facile on the Au/Fe(OH)$_3^*$ catalyst, and the Fe sites become free for oxygen adsorption by the water–gas shift reaction, allowing further reaction to occur. Andreeva's studies on low-temperature water–gas shift over gold catalysts [45,46] prepared by a modified deposition–precipitation technique (i.e., gold hydroxide deposited on freshly precipitated metal hydroxide) showed a large variation in activity depending on the nature of support. Thus, the temperature for 50% conversion was 423 K for the Au/FeO_3 catalyst with 3.5-nm-diameter Au particles, but 573 K for the Au/TiO_2 catalyst with Au particle diameters <3 nm. Moreover, a recent DRIFTS study combined with mass spectrometry showed that the water–gas shift reaction occurred even at room temperature over an Au/Fe_2O_3 catalyst obtained by co-precipitation, with an Au loading of 4.48% and Au particle sizes of 3–5 nm (mean size, 2.8 nm) [47]. The adsorptive mechanism comprising CO adsorption on Au particles, formation of carbonates and bicarbonates at the Au–Fe_2O_3 interface, and their decomposition to CO_2 appears to prevail at low temperature, whereas at around 473 K, the regenerative mechanism is dominant. Under these conditions, the catalyst support Fe_2O_3 is easily reducible in the presence of Au. The study also revealed that the Au particles are essential for H_2 production and the reoxidation step involving H_2O as the reactant. The greatest effect is associated with the presence of a higher concentration of low-coordinated sites on the surface of smaller particles on the Au/Fe(OH)$_3^*$ catalyst, which leads to a higher stabilization of reaction intermediates, such as CO or oxygen, on the surface of gold.

4. Conclusion

The TAP study revealed that moisture in the reactant gas had different effects on the activity of Au/Ti(OH)$_4^*$ and Au/Fe(OH)$_3^*$ catalysts with respect to CO oxidation. Whereas the activity of the Au/Ti(OH)$_4^*$ catalyst was totally suppressed irrespective of the water content between 200 and 1000 ppm, no effect was observed for the Au/Fe(OH)$_3^*$ catalyst. When the CO:O_2 ratio was 1:1 in the absence of water, CO oxidation was characterized by a two-peak feature in the CO response curve, with only one peak seen in the presence of water. At a CO:O_2 ratio of 1:3, the CO response curve exhibited one peak with a peak

shift to shorter time. These TAP results indicate that CO and water absorbed competitively and that water blocked the adsorption sites for O_2 irreversibly on Au/Ti(OH)$_4^*$ and reversibly on Au/Fe(OH)$_3^*$. The CO adsorption was weak and reversible, whereas O_2 adsorption was strong and irreversible, but weaker on Au/Fe(OH)$_3^*$ than on Au/Ti(OH)$_4^*$.

Acknowledgments

This work was supported by Core Research for Evolutional Science and Technology (CREST) of the Japan Science and Technology Corporation (JST). The authors thank Dr. H. Liu and Dr. A.I. Kozlov for preparing the catalysts.

References

[1] M. Haruta, T. Kobayashi, H. Sano, N. Yamada, Chem. Lett. 16 (1987) 405–408.
[2] G.C. Bond, D.T. Thompson, Catal. Rev. Sci. Eng. 41 (1999) 319–388.
[3] G.C. Bond, Gold Bull. 34 (2001) 117–140.
[4] M. Haruta, M. Daté, Appl. Catal. A 222 (2001) 427–437.
[5] M. Haruta, CATTECH 6 (2002) 102–115.
[6] C.W. Corti, R.J. Holliday, D.T. Thompson, Gold Bull. 35 (2002) 111–136.
[7] D.T. Thompson, Appl. Catal. A 243 (2003) 201–205.
[8] H.H. Kung, M.C. Kung, J. Catal. 216 (2003) 425–432.
[9] M. Haruta, J. New Mater. Electrochem. Syst. 7 (2004) 163–172.
[10] M. Haruta, Gold Bull. 37 (2004) 27–36.
[11] C.W. Corti, R.J. Holliday, D.T. Thompson, Appl. Catal. A 291 (2005) 253–261.
[12] J.D. Henao, T. Caputo, J.H. Yang, M.C. Kung, H.H. Kung, J. Phys. Chem. B 110 (2006) 8689–8700.
[13] F. Cosandey, T.E. Madey, Surf. Rev. Lett. 8 (2001) 73–93.
[14] P. Pyykko, Angew. Chem. Int. Ed. 43 (2004) 4412–4456.
[15] A. Cho, Science 299 (2003) 1684–1685.
[16] M. Valden, X. Lai, Dz.W. Goodman, Science 281 (1998) 1647–1650.
[17] M. Mavrikakis, P. Stoltze, J.K. Norskov, Catal. Lett. 64 (2000) 101–106.
[18] H.G. Boyen, G. Kastle, F. Weigl, B. Koslowski, C. Dietrich, P. Ziemann, J.P. Spatz, S. Riethmuller, C. Hartmann, M. Moller, G. Schmid, M.G. Garnier, P. Oelhafen, Science 297 (2002) 1533–1536.
[19] S.K. Shaikhutdinov, R. Meyer, M. Naschitzki, M. Bäumer, H.-J. Freund, Catal. Lett. 86 (2003) 211–219.
[20] Y. Xu, M. Mavrikakis, J. Phys. Chem. B 107 (2003) 9298–9307.
[21] R.J. Davis, Science 301 (2001) 926–927.
[22] Q. Fu, H. Saltsburg, M. Flytzani-Stephanopoulos, Science 301 (2003) 935–938.
[23] N.M. Gupta, A.K. Tripathi, J. Catal. 187 (1999) 343–347.
[24] N.M. Gupta, A.K. Tripathi, Gold Bull. 34 (2001) 120–128.
[25] S.T. Daniells, A.R. Overweg, M. Makkee, J.A. Moulijn, J. Catal. 230 (2005) 52–65.
[26] M. Daté, M. Haruta, J. Catal. 201 (2001) 221–224.
[27] M. Haruta, T. Takase, T. Kobayashi, S. Tsubota, in: S. Yoshida, N. Takezawa, T. Ono (Eds.), Catalytic Science and Technology, vol. 1, Kodansha, Tokyo, 1991, pp. 331–335.
[28] E.D. Park, J.S. Lee, J. Catal. 186 (1999) 1–11.
[29] C.K. Costelo, M.C. Kung, H.-S. Oh, Y. Wang, H.H. Kung, Appl. Catal. A 232 (2002) 159–168.
[30] D.A.H. Cunningham, W. Vogel, M. Haruta, Catal. Lett. 63 (1999) 43–47.
[31] G.C. Bond, D.T. Thompson, Gold Bull. 33 (2000) 41–51.
[32] H.-S. Oh, C.K. Costelo, C. Cheung, H.H. Kung, M.C. Kung, Stud. Surf. Sci. Catal. 139 (2001) 375–381.
[33] M.A. Bollinger, M.A. Vanice, Appl. Catal. B 8 (1996) 417–443.
[34] G.B. Raupp, J.A. Dumisec, J. Phys. Chem. 89 (1985) 5240–5246.
[35] H. Liu, A.I. Kozlov, A.P. Kozlova, T. Shido, Y. Iwasawa, Phys. Chem. Chem. Phys. 1 (1999) 2851–2860.
[36] A.P. Kozlova, A.I. Kozlov, S. Sugiyama, Y. Matsui, K. Asakura, Y. Iwasawa, J. Catal. 181 (1999) 37- 48 .
[37] H. Liu, A.I. Kozlov, A.P. Kozlova, T. Shido, K. Asakura, Y. Iwasawa, J. Catal. 185 (1999) 252–264.
[38] M. Olea, M. Kunitake, T. Shido, K. Asakura, Y. Iwasawa, Bull. Chem. Soc. Jpn. 74 (2001) 255–265.
[39] M. Olea, M. Kunitake, T. Shido, Y. Iwasawa, Phys. Chem. Chem. Phys. 3 (2001) 627–631.
[40] Y. Yuan, A.P. Kozlova, K. Asakura, H. Wan, K. Tsai, Y. Iwasawa, J. Catal. 170 (1997) 191–199.
[41] Y. Yuan, K. Asakura, A.P. Kozlova, H. Wan, K. Tsai, Y. Iwasawa, Catal. Today 44 (1998) 333-342 .
[42] A.I. Kozlov, A.P. Kozlova, K. Asakura, Y. Matsui, T. Kogure, T. Shido, Y. Iwasawa, J. Catal. 196 (2000) 56–65.
[43] J.T. Gleaves, G.S. Yablonskii, P. Phanawadee, Y. Shuurman, Appl. Catal. A 160 (1997) 55–88.
[44] N. Lopez, T.V.W. Jansen, B.S. Clausen, Y. Xu, M. Mavrikakis, T. Bligaard, J.K. Nørskov, J. Catal. 223 (2004) 232–235.
[45] Ed. Andreeva, V. Idakiev, T. Tabakova, A. Andreev, J. Catal. 158 (1996) 354–355.
[46] D. Andreeva, Gold Bull. 35 (2002) 82–88.
[47] B.A.A. Silberova, G. Mul, M. Makkee, J.A. Moulijn, J. Catal. 243 (2006) 171–182.